Evaluation of the Energetics of the Concerted Acid-Base Mechanism in Enzymatic Catalysis: The Case of Ketosteroid Isomerase

Stephen D. Fried and Steven G. Boxer

Supplementary Information

Contents:

Supplementary Methods

Preparation and isolation of KSI. All experiments were conducted on the Ketosteroid Isomerase (KSI) from *Pseudomonas putida* (pKSI) with the mutation D40N. The protocol employed was similar to that reported previously.[31]

A pKK223-3 construct containing the open-reading frame for the KSI gene along with a Carbenicillin resistance gene was transformed into BL21-AI competent *E. coli* cells (Stratagene). Single colonies were selected from an agar plate treated with Carbenicillin, and then grown in 10 mL starter cultures consisting of LB broth (8 h, 37.5 ^{o}C) with 100 µg/mL Carbenicillin. The starter cultures were transferred to typically 2 × 1 L of TB broth with 100 µg/mL Carbenicillin. The expression culture was incubated at 37.5 ^{o}C, 200 rpm. After 1 h, IPTG was added to 0.5 mM to induce expression, and growth/expression continued overnight for an additional ca. 15 h. Cells were harvested by centrifugation, resuspended in 40 mM KP_i (1 mM EDTA, 2 mM DTT, 1-2 mg bovine DNAse), and lysed by homogenization. The lysate was centrifuged again, and the supernatant was filtered once with a .45 µm filter then with a .22 µm filter. The filtered lysate was loaded onto a custom-designed deoxycholate-based affinity column; nearly-pure KSI^{D40N} was eluted off the column in 50% EtOH (vol/vol). Eluted protein was exchanged with buffer to reduce EtOH to 10% (vol/vol) by dilution-reconcentration cycles with centrifugal concentrators with a 10,000 molecular weight cutoff (Amicon). Afterwards, it was further purified by gel-filtration chromatography using an FPLC set-up (GE Healthcare). Pure KSI^{D40N} was concentrated to high concentrations (1-8 mM) using centrifugal concentrators of various sizes but always with a 10,000 molecular

weight cut-off. A typical purified yield of KSI^{D40N} was 150-200 mg/L. KSI solutions at concentrations >2 mM tend to be quite viscous and occasionally precipitate during concentration. Concentrations were measured by UV-Vis spectrophotometry using a Perkin-Elmer Lambda with the extinction coefficient, $\varepsilon_{280} = 16.6\ mM^{-1}\ cm^{-1}$. Highly concentrated KSI slowly precipitates, and so when not in use, stocks were always flash-frozen in liquid N_2 and stored at -80 ^{o}C.

^{13}C NMR Spectroscopy. All samples were prepared by mixing appropriate amounts of KSI^{D40N} (40 mM KP_i), isotopically-labeled ligand (~100 mM in DMSO), 17.5 µL D_2O (Cambridge Isotopes), and buffer to a volume of 350 µL. The final concentration of KSI^{D40N} was always 1.5 mM. This solution was transferred to a 5 mm Shigemi symmetrical microtube (Shigemi Inc.) susceptibility-matched to D_2O with the proper bottom-length for a Bruker probe. Air bubbles trapped beneath the Shigemi tube insert were removed by firmly depressing the insert into the sample solution to squeeze the bubbles up past the insert. Spectra were acquired at the Stanford Magnetic Resonance Laboratory on a Bruker Avance 500 MHz spectrometer running TopSpin v1.3, and equipped with a 10 mm broadband observe probe. One-dimensional carbon-13 spectra were obtained at 25˚C using a single pulse sequence (90˚ hard-pulse) with no proton decoupling during detect, 2 s pre-scan delay, 33 kHz spectral window and 99k total data points. Between 2000-4000 scans were averaged to furnish the FIDs, which were processed in Topspin using a 10 Hz line broadening function and auto-phased. The observed resonance chemical shifts were determined using the Topspin peak-picking option. The spectra were referenced to an external sample of 200 mM TSP (40 mM KP_i,

5% vol/vol D_2O) set to 0 ppm. To perform a ligand concentration series, additional ligand was added in small volumes of DMSO to the same sample. This manipulation was done by removing the sample contents with a long Pasteur pipette from the Shigemi tube into a microcentrifuge tube. The additional ligand (typically <1 μL) was added, and mixed by aspiration. The contents were then delivered back to the Shigemi tube.

Preparation of 4-fluorophenol-2,6-*d*$_2$. 4-fluorophenol-2,6-d_2 (4F*d*2) was prepared by a method based on that of Perrin and Dong.[47] In greater detail, 4-fluorophenol (Sigma-Aldrich, 1.12 g, 10 mmol) was added to an oven-dried round bottom flask containing 6.4 g of 1:1 (w/w) D_2SO_4:D_2O. The solution was heated in an oil bath at 75˚C, and stirred with a magnetic stir bar. After 6 h, the mixture was dropped slowly onto ice and extracted 3 times with diethyl ether (15 mL). The combined organics were dried over Na_2SO_4 and reduced by rotary evaporation, furnishing an orange-colored oil. The oil was re-dissolved in 6.4 g of 1:1 (w/w) D_2SO_4:D_2O and the procedure was repeated. Rotary evaporation led to an oily residue that could not be further reduced. The oil was allowed to stand unsealed overnight in the round bottom flask in the fume hood, during which some crystallites appeared. When the residue was placed on top of the crystallite (by reorienting the round-bottom flask), the product immediately crystallized into light pink-colored needles (.50 g, 45% yield). Characterization by ^{1}H NMR and ^{19}F NMR was consistent with the specifications of ref. 47. Other phenols studied by IR were purchased from Sigma-Aldrich, and used with no further purification. Additionally, we note that the pK_a of 4-fluorophenol-2,6-d_2 differs from that of 4-fluorophenol by only .01 units.[47]

Preparation of [1-^{13}C]phenols. [1-^{13}C]4-nitrophenol was prepared from [2-^{13}C]acetone (Cambridge Isotopes, 50 mg, .85 mmol) according to Walker *et al.*[48] except at ca. 1/100th of the scale. 41.8 mg of [1-^{13}C]4-nitrophenol was obtained as a brown-yellow powder (36% yield). [1-^{13}C]phenol was purchased from Cambridge Isotopes, and used with no further purification.

Supplementary Results

^{13}C NMR spectra of [1-^{13}C]phenols

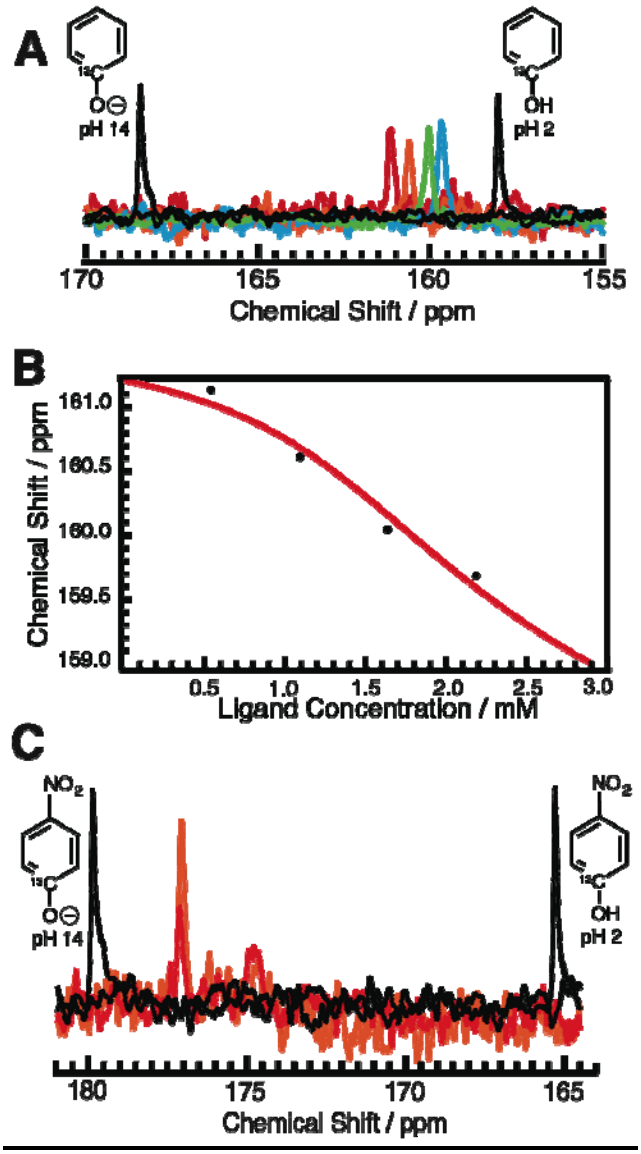

Figure S1. (A) ^{13}C NMR spectra of phenol (10 mM; 5% D_2O) in 1 M KOH and .01 mM HCl (black) and KSI^{D40N}•phenol (color) in 40 mM KP_i, pH 7.2. [KSI] = 1.5 mM; [phenol] = .54 mM (red), 1.1 mM (orange), 1.6 mM (green), 2.2 mM (blue). (B) Plot of ^{13}C chemical shift vs. concentration of phenol. The data are fit to eq (S1). (C) ^{13}C NMR spectra of nitrophenol (10 mM; 5% D_2O) in 1 M KOH and .01 mM HCl (black) and

KSI^{D40N}•nitrophenol (color) in 40 mM KP_i, pH 7.2. [KSI] = 1.5 mM; [phenol] = .50 mM (red), and 1.0 mM (orange).

IR Spectra of 4-fluoro-3-methylphenol

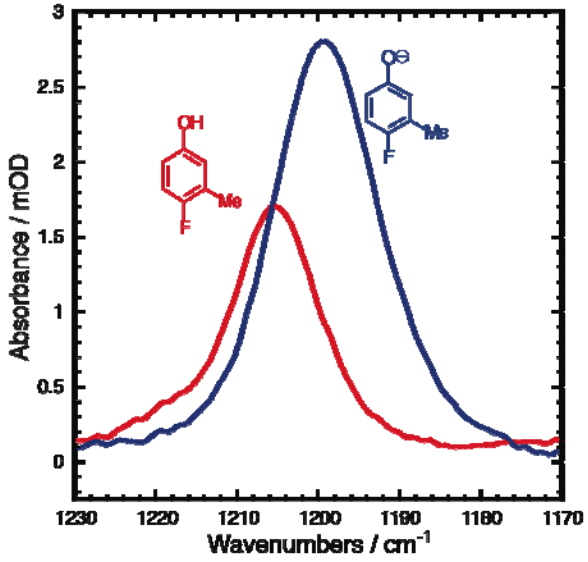

Figure S2. 4-Fluoro-3-methylphenol (3 mM, pH 2, .01 M HCl) in red, and 4-fluoro-3-methylphenoxide (3 mM, pH 14, 1 M KOH) in blue. The ionization-induced shift of the C-F stretch band is small relative to the peaks' width, so this ligand is not a useful probe of ionization state.

Table S1. ^{13}C NMR chemical shifts

[1-^{13}C]Phenol			[1-^{13}C]4-Nitrophenol		
System [a]	Condition	δ / ppm	System [a]	Condition	δ / ppm
Aqueous	pH 2	158.06	Aqueous	pH 2	165.30
	pH 14	168.46		pH 10	179.79
KSI-bound	.54 mM	161.14		pH 14	179.92
	1.1 mM	160.61	KSI-bound	.50 mM	177.13
	1.6 mM	160.05		1.0 mM	177.07
	2.2 mM	159.68			

[a] Details of the system conditions are described in the caption of Figure S1

Table S2. Supplementary FTIR data

4-fluoro-3-methylphenol $\tilde{\nu}$ (C-F)			
system [a]	peak position / cm^{-1}	fwhm / cm^{-1}	intensity
pH 2	1205.4 ± .2	12.60	1.6
pH 14	1199.3 ± .1	15.53	2.8

[a] Details of the system conditions are described in caption of Figure S2

Table S3. All FTIR data of KSI^{D40N}•4F*d*2

4-fluorophenol-d_2 $\tilde{\nu}$(C-F)								
[KSI] / mM	[ligand] / mM	f_{bound} [a]		Peak Position / cm^{-1}	FWHM / cm^{-1}	Peak Max / mOD	f_{obs} [b]	f [b]
7.4	3.0	.97	Peak 1	1188.5 ± .3	8.81	1.1	.29	.30
			Peak 2	1171.1 ± .5	7.18	1.0		
			Fit 1 [d]	1187.9	12.42	1.11		
			Fit 2 [d]	1171.9	10.58	1.00		
4.7	3.0	.92	Peak 1	1188.2 ± .2	10.94	1.3	.26	.28
			Peak 2	1172.3 ± .2	7.52	1.2		
			Fit 1 [d]	1187.9	13.63	1.28		
			Fit 2 [d]	1171.9	9.57	1.20		
4.7	5.0	.80	Peak 1	1189.0 ± .1	9.64	2.4	.24	.29
			Peak 2	1173.2 ± .4	8.97	1.1		
			Fit 1 [d]	1188.9	10.41	2.39		
			Fit 2 [d]	1173.4	13.03	1.14		

Corresponds to the spectra in Figure 4. [a] The fraction of ligand that is bound to KSI. Calculated using the K_D of 150 μM. [b] f_{obs} is the fraction of ligand ionized; f is the fraction of *bound* ligand that is ionized, determined by subtracting the contribution from unbound ligand. See analysis in the main text.

Supplementary Discussion

Interpretation of ^{13}C NMR data. The ^{13}C chemical shift of the C1 carbon in phenol is a sensitive probe of ionization state (168.46 ppm in the ionized stated and 158.06 ppm in the neutral state, Figure S1A, black traces), allowing one to distinguish between the two tautomeric forms of the internal proton transfer. The binding constant of phenol at pH 7.2 (K_D = 150 μM) is such that NMR is not amenable to the set of enzyme and ligand concentrations needed for the ligand to be quantitatively bound. Nevertheless, a series of measurements (Figure S1A, colored traces) at several ligand concentrations can be fit to

$$\delta_{obs} = f_{bound}(K_D, \text{pH}, [\text{KSI}], [\text{phenol}])\ \delta_{bound} + (1 - f_{bound})\ \delta_{free} \qquad \text{(S1)}$$

where f_{bound} is the fraction of ligand that is bound, δ_{bound} and δ_{free} are the basis chemical shifts of [1-^{13}C]phenol in the bound and free form, respectively, and δ_{obs} is the observed peak position for a given ligand concentration. f_{bound} can be calculated in terms of specified quantities, and δ_{bound} and δ_{free} can be extracted by fitting eq S1 to the data. Figure S1B shows that eq S1 is a satisfactory model, from which we can extract the basis chemical shift for the bound state (δ_{bound} = 161.67 ppm). At no concentration is phenol ever quantitatively bound, and therefore the intercept of this plot does not occur at 161.67 ppm.

The validity of eq S1, which asserts a linear dynamic averaging between the bound and free states of phenol, is based on the separation of timescales between the binding kinetics ($k_{off} \sim 10^4$ s^{-1}) and the chemical shift timescale associated with the ~5 ppm of dispersion at ^{13}C's Larmor frequency (10^2-10^3 Hz). The value that δ_{bound} assumes

can be approximated as resulting from a superposition of protonated and neutral forms of phenol when in the KSI^{D40N} active site, according to eq S2:

$$\delta_{bound} = f\delta_{ionized} + (1 - f)\ \delta_{neutral} \qquad (S2)$$

where $\delta_{ionized}$ and $\delta_{neutral}$ are the basis chemical shifts of [1-^{13}C]phenol in the ionized and protonated states respectively (black traces in Figure S1A), and f is the fraction of bound ligand ionized, as defined previously. Eq S2 presumes yet another separation of timescales: this time between the binding kinetics ($k_{off} \sim 10^4$ s^{-1}) and the rate constant of the internal proton transfer that relates the two tautomeric forms, E-O$^-$•HO-L and E-OH•$^-$O-L ($k \sim 10^{11}$ s^{-1} based on the peak separation observed by IR, see Figure 2F). In other words, the bound state as represented by δ_{bound} reflects the weighted average ionization state of [1-^{13}C]phenol whilst it is bound to KSI^{D40N}. Therefore according to eq (S2), δ_{bound} determines f with no free parameters, and we calculate $f = 0.35$.

This interpretation assumes that δ_{bound} reflects only ionization; on the other hand, one must be aware of the possible contribution to δ_{bound} due to the active site environment, that is, due to electric fields (solvation) and magnetic fields (ring currents), which may confound eq S2 and a simple interpretation of δ_{bound}. As a telling example of this complication, we performed an identical experiment with the ligand [1-^{13}C]4-nitrophenol (Figure S1C). 4-nitrophenol has much stronger affinity (K_D = 2 μM [31]) and is known to bind quantitatively in the anionic form (i.e., $f = 1$) from UV-Vis spectroscopy.[31] Nevertheless, as seen in Figure S1C, its chemical shift bound to KSI^{D40N} is about 3 ppm off from the value expected if one were to assume the only contribution to the chemical shift were ionization (compare the red or orange trace to the fully ionized basis peak at 179.92 ppm). If this also applied to phenol, the conceivable uncertainty in f would be

very high (0.35 ± 0.30). These observations highlight the difficulty in identifying incisive probes of the internal proton transfer for the general reason that environmental effects are convolved with ionization by many spectroscopic observables. The analysis presented illustrates a general limitation of NMR methods, and explains the disagreement between the IR data presented in the main text and the ^{19}F NMR experiments in ref 31. We note further that the ^{19}F nucleus is even more sensitive to environment (as quantified by the shielding polarizability[49]) than ^{13}C, rendering eq S2 even less valid, and rendering ^{19}F NMR a less faithful reporter of ionization state.

4-cyanophenol binds as an anion. While 4F*d*2 (solution pK_a = 10.0) binds to the active site of KSI^{D40N} as a mixture of the protonated and deprotonated forms, other phenols whose solution pK_as are lower are expected to bind largely as anions.[29,30] A previous study determined that 4-nitrophenol (pK_a 7.14) binds as an anion,[31] and Figure 3 shows that 4-cyanophenol (pK_a 7.95) binds exclusively as an anion, as expected. We performed these studies at a higher pH in the event that if some 4-cyanophenol were unbound, it would be ionized, so neutral 4-cyanophenol would have to be due to action of the KSI active site. In contrast, UV-Vis spectroscopy and ^{19}F NMR studies in ref. 31 came to the conclusion that phenols of all pK_a bind as anions, which is inconsistent with the present results as well as forthcoming ones. As discussed in the main text, UV-Vis spectroscopic methods suffer from the spectral overlap of protonated and deprotonated forms. NMR methods suffer from the convolution of environmental and ionization effects in the chemical shift, *vide supra*.

Supplementary References

47. Perrin, C .L.; Dong, Y. *J. Am. Chem. Soc.* **2007,** 129, 4490-4497.

48. Walker, T. E.; Matheny, C.; Storm, C.B.; Hayden, H. *J. Org. Chem*. **1986**, 51, 1175-1179.

49. Augspurger, J. D.; Dykstra, C. E. *J. Am. Chem. Soc.* **1993**, 115, 12016-12019.